Isoscalar spin excitation in ^{90}Zr and ^{208}Pb

C. Djalali,[1,2] M. Morlet,[2] N. Marty,[2,*] J. Van de Wiele,[2] A. Willis,[2] F. T. Baker,[3] L. Bimbot,[2] C. Glashausser,[4] J. Guillot,[2] H. Langevin-Joliot,[2] L. Rosier,[2] and E. Tomasi-Gustafsson[5]

[1]*Department of Physics and Astronomy, University of South Carolina, Columbia, South Carolina 29208*

[2]*CNRS-IN2P3, Institut de Physique Nucléaire, Orsay, BP N° 1, F-91406, France*

[3]*Department of Physics and Astronomy, University of Georgia, Athens, Georgia 30602*

[4]*Department of Physics and Astronomy, Rutgers University, Piscataway, New Jersey 08854*

[5]*DAPNIA-SPhN and Laboratoire National Saturne, CEN Saclay, F-91191 Gif-sur-Yvette Cedex, France*

(Received 26 March 1998)

Isoscalar spin-transfer excitations have been measured in ^{90}Zr and ^{208}Pb by inelastic scattering of vector and tensor polarized 400 MeV deuterons in an excitation energy range from 2.5 to 43 MeV and 2.3 to 23 MeV, respectively. For ^{90}Zr, spin excitations were found between 7.5 and 10.7 MeV and in a large structure in the continuum (18 to 28 MeV). For ^{208}Pb, spin excitations were found at 3.55 and 5.85 MeV, between 6.5 and 11 MeV, and spread over the continuum. Elastic scattering cross sections and vector and tensor analyzing powers were measured between 3.4 and 24° for Zr and Pb, and optical potential parameters were derived. The experimental results are compared to DWIA/RPA calculations. The transition densities used are generated using the continuum random phase approximation. [S0556-2813(99)06301-3]

PACS number(s): 25.45.De, 24.70.+s, 27.60.+j, 27.80.+w

I. INTRODUCTION

Spin excitations have been extensively studied in many nuclei from ^{12}C to ^{208}Pb using different reactions such as (p,n) and $(^3\mathrm{He},t)$ charge exchange [1–4] and electron [5] and proton inelastic scattering [6–11]. However, very few isoscalar spin states are known, because all of these reactions excite either exclusively or essentially spin isovector transitions. In inelastic proton scattering, isovector spin transitions are favored because in the nucleon-nucleon interaction, the isovector spin force is at least three times larger than the isoscalar one. As deuteron inelastic scattering can excite only isoscalar transitions, it is probably the simplest and best probe to study isoscalar spin excitations. A detailed study of polarization transfer in inelastic scattering of intermediate energy deuterons allowed us to find a robust observable that uniquely selects $S=1$, $T=0$ transitions. This signature was successfully used in mapping out the isoscalar spin strength in ^{12}C [12,13] and ^{40}Ca [14]. These results are described at length in Ref. [15], where the theoretical issues are also extensively explored. Previously unknown $S=1$, $T=0$ transitions have been observed at low excitation energies in both nuclei and the spin strength distribution has been measured in the continuum up to 50 MeV.

The purpose of the present work is to extend the study of isoscalar spin transitions to medium and heavy nuclei. We chose to study ^{90}Zr and ^{208}Pb because these two nuclei have been extensively studied by different reactions and in ^{208}Pb an isocalar 1^+ state has been observed at 5.85 MeV. Using the measured spin-flip probability S_d^y and some approximations (described in Sec. II), we will extract from the measured cross section, the $S=0$ and $S=1$ cross sections.

The data are compared to distorted wave impulse approximation (DWIA) calculations done with transition densities obtained within the continuum second random phase approximation (RPA). These predictions should give us a tool for understanding the isoscalar spin response in the continuum of nuclei. We also performed elastic scattering measurements in order to derive optical potential parameters needed for our distorted wave calculations.

In Sec. II simple expressions for the spin observables are given and the different derived quantities are explained. In Sec. III a brief description of the continuum random phase approximation calculations is given. Section IV contains a brief description of the experimental setup. The experimental results are given and discussed in Sec. V; the summary and conclusions are presented in Sec. VI.

II. SIGNATURE FOR SPIN TRANSITION AND DERIVED QUANTITIES

It has been shown in Refs. [12,14,15] that in $(\vec{d},\vec{d}')$ scattering a good signature for isoscalar spin excitation is a quantity closely related to the spin-flip probability:

$$S_d^y=\frac{4}{3}+\frac{2}{3}A_{yy}-2K_y^{y'}. \tag{2.1}$$

A_{yy} is the tensor analyzing power of the reaction and $K_y^{y'}$ is the vector spin transfer coefficient (the lower index refers to the incident beam, the upper to the scattered beam). Double spin-flip is suppressed at low momentum transfer and to a very good approximation S_d^y is equal to zero for spin transfer $S=0$ and it is different from zero for spin transfer $S=1$. The detailed algebra relating the different asymmetry, polarization, and spin transfer observables is given in Ref. [16]. The complete microscopic description of deuteron-nucleus scattering based on the distorted wave impulse ap-

*Deceased.

proximation and of the signature for spin-flip transitions can be found in Ref. [15]. We will briefly recall some simple definitions.

Let σ_{00}^A and σ_{10}^A be respectively the isoscalar cross sections for a spin transfer of 0 and 1 to the nucleus. Assuming S_d^y is equal to the isoscalar spin-flip probability (probability to have a change of one unit in the deuteron-spin projection on the y axis normal to the scattering plane), we have

$$S_d^y=(\alpha^A\sigma_{10}^A)/(\sigma_{00}^A+\sigma_{10}^A), \tag{2.2}$$

where α^A is defined as the spin-flip probability for a pure $S=1$ transition ($\sigma_{00}^A=0$). The value of α^A depends on nuclear structure and is therefore model dependent. It cannot be determined experimentally in the continuum, since $S=1$ states cannot be isolated there. However, in the continuum where different multipolarities mix, we expect an average value of α^A very close to α^{free} calculated for free deuteron-nucleon (d-N) scattering. Making this assumption, we can factorize the cross sections as

$$\sigma_{i0}^A=N_{\text{eff}}f_{i0}\sigma_{i0}^{\text{free}}, \tag{2.3}$$

where N_{eff} is the effective number of participating nucleons (supposed to be the same in both channels), f_{i0} the isoscalar nuclear response in the spin channel i, and $\sigma_{i0}^{\text{free}}$ the d-N scattering cross section calculated for the momentum transfer $\vec{q}$ of the deuteron-nucleus inelastic scattering. Then

$$S_d^y=(f_{10}\sigma_{10}^{\text{free}}\alpha^{\text{free}})/(f_{10}\sigma_{10}^{\text{free}}+f_{00}\sigma_{00}^{\text{free}}). \tag{2.4}$$

From the above relations, one can derive for the $S=1$ cross section the following expression:

$$\sigma_{10}^A=\frac{1}{\alpha^{\text{free}}}\frac{d\sigma}{d\Omega}S_d^y, \tag{2.5}$$

where $d\sigma/d\Omega=\sigma_{00}^A+\sigma_{10}^A$ is the experimental cross section. It should be noted that the magnitudes of σ_{00}^A and σ_{10}^A depend on the approximation $\alpha^A\approx\alpha^{\text{free}}$.

The relative isoscalar spin response $\mathcal{R}_1^0$ is just the ratio of the isoscalar spin-one response to the isoscalar total response and it is given by

$$\mathcal{R}_1^0=\frac{f_{10}}{f_{10}+f_{00}}. \tag{2.6}$$

$\mathcal{R}_1^0$ is a nuclear structure quantity, a measure of the relative strength of isoscalar spin-dependent matrix elements at different excitation energies and momentum transfers. Note that a value of 0.5 for $\mathcal{R}_1^0$ would be expected if the nucleus responded like a noninteracting Fermi gas. One of the major objectives of this work is that of determining $\mathcal{R}_1^0$ experimentally.

From Eqs. (2.4) and (2.6) we obtain

$$\mathcal{R}_1^0=\frac{S_d^y}{S_d^y[1-(\sigma_{10}^{\text{free}}/\sigma_{00}^{\text{free}})]+\alpha^{\text{free}}(\sigma_{10}^{\text{free}}/\sigma_{00}^{\text{free}})}. \tag{2.7}$$

This equation is used to determine the *experimental* values of $\mathcal{R}_1^0$, but the *theoretical* values of $\mathcal{R}_1^0$ can be determined from Eq. (2.6) without reference to spin-flip probabilities or α. In the PW or DW calculations based on the RPA, all σ_{ST}^A are calculated individually and Eqs. (2.3) and (2.6) can be applied directly.

When presenting the data, we will always show two sets of spectra. The first set, called directly measured quantities, consists of the differential cross section, the signature and the spin-flip cross section as a function of excitation energy. The spin-flip cross section is just the product of the cross section and the measured signature. The second set, called derived quantities, involves the assumptions mentioned above and consists of the $S=1$ cross section, the $S=0$ cross section and the relative spin response as a function of excitation energy. All of these spectra are compared to the DWIA/RPA.

III. RPA DESCRIPTION

Transition densities used in the distorted wave calculations of observables were generated using the continuum random phase approximation (RPA) [17–20] with the approximate treatment of 2p-2h contributions of Smith and Wambach [21]. The form of the residual interaction used in the RPA calculations was a zero-range Landau-Migdal interaction [22]:

$$V_{\text{ph}}(\vec{r})=C_0(f_0(r)+g_0\vec{\sigma}\cdot\vec{\sigma}')\delta^3(\vec{r}), \tag{3.1}$$

with $C_0=150$ MeV fm^3. The $S=0$, $T=0$ part of the interaction, $f_0(r)$, is density dependent. For ^{208}Pb, the parameters of $f_0(r)$ were chosen such that the compressibility of nuclear matter and the position of the first 2^+ state (4.1 MeV) were reproduced by the RPA calculations. The giant quadrupole resonance is predicted to be at about 9.5 MeV, about 1 MeV lower than experiment, and the giant monopole resonance is predicted to be at about 12.5 MeV, again about 1 MeV lower than experiment. For ^{90}Zr the parameters of $f_0(r)$ were chosen such that the compressibility of nuclear matter and the position of the giant quadrupole resonance (about 14.5 MeV) were reproduced by the RPA calculations. The parameter g_0, which determines the $S=1$, $T=0$ part of the residual interaction, is believed to be small [24,25] and has been set to zero in all calculations shown here. The effect of the parameter g_0 is to shift the isoscalar-spin spectrum and our choice of zero has negligible effects on the calculations when compared to any other reasonable estimate of its value.

The methods used to generate the hole states required in the RPA calculations were different for the two nuclei studied here as described below.

A. ^{208}Pb

For ^{208}Pb a mean-field potential of the form

$$V(r)=V_0f(r)+\frac{1}{r}\frac{df}{dr}V_{LS}\vec{\sigma}\cdot\vec{l}+\frac{1}{2}(1-\tau_z)V_c(r) \tag{3.2}$$

was used, where $f(r)=[1+\exp(r-r_0A^{1/3}]^{-1}$. The parameters of this potential were determined separately for protons and neutrons by performing χ^2 minimization fits to the experimental root mean square (rms) radius and experimental single-particle energies of orbitals near the Fermi surface. The rms radius was taken as the electron scattering value of

5.5 fm [23] for both proton and neutron wells. The neutron orbitals fitted were the $3p_{1/2}$, $3p_{3/2}$, $2f_{5/2}$, $2f_{7/2}$, and $1i_{13/2}$. The proton orbitals fitted were the $3s_{1/2}$, $2d_{3/2}$, $2d_{5/2}$, and $1h_{11/2}$. In these searches all diffusenesses were held constant at 0.67 fm and the Coulomb and central radii were held equal to each other. The depths and radii of the central and spin-orbit potentials were varied simultaneously.

B. ^{90}Zr

For ^{90}Zr the hole states required in the continuum RPA calculations were generated using a Hartree-Fock density matrix expansion (DME) [26] calculation. The resulting ground-state wave function has a full $2p_{1/2}$ proton orbital and an empty $1g_{9/2}$ proton orbital. As explained in Ref. [15], the resulting energy-weighted sum rule (EWSR) for DME calculations differs from its usual form,

$$m_\alpha^1 = \int d\vec{r} \frac{\hbar^2 (\nabla P_\alpha(\vec{r}))^2}{2M} \rho_0(\vec{r}), \tag{3.3}$$

where P_α is the probing function, M is the nucleon mass, and ρ_0 is the ground state density. The difference is that M is replaced by an r-dependent effective mass which results in all EWSR values being increased to about 140% of the usual values. However, it is known that conservation of particle number requires that the EWSR must be the value given by Eq. (3.3) for the $S=0$, $T=0$ channel. In the present work the transition densities for this channel have been scaled down to preserve 100% of the usual EWSR; the $S=1$, $T=0$ channel, however, has not been rescaled. Although this is somewhat arbitrary, there is evidence that channels other than the scalar-isoscalar channel overexhaust the sum rule; for example, the giant dipole resonance is generally acknowledged to exhaust more than 150% of the EWSR and there is evidence [9,11] that the isovector spin dipole resonance also contains substantially more than 100% of the EWSR.

This rescaling is only required for ^{90}Zr since the ^{208}Pb calculations did not use Hartree-Fock wave functions.

IV. EXPERIMENTAL SETUP AND PROCEDURE

What follows is a brief review of the experimental set-up and techniques used in the present experiment; for a detailed description of the techniques used, the reader is referred to Ref. [13].

The data were taken at the Saturne National Laboratory, using the facility's 400 MeV polarized deuteron beam, the high-resolution magnetic energy-loss spectrometer SPES1 [27] and the acquisition system described in Ref. [28]. The polarization of the scattered deuterons was measured with the large acceptance focal plane polarimeter POMME. The use of POMME as a vector polarimeter for deuterons is described in detail in Refs. [29,30]. The energy resolution (due mostly to target thickness) in the focal plane of SPES1 was of the order of 200 keV (FWHM) using a 40 mg/cm^2 ^{90}Zr and a 20 mg/cm^2 ^{208}Pb target.

The experiment made use of two different modes of beam polarization. In the first mode (the ''four-state'' mode), the beam is vector and tensor polarized in four different states, the polarization state changing with each beam pulse. The p_y and p_{yy} values of the beam were measured regularly with the low energy polarimeter [31], they were found to be stable within a statistical uncertainty of 3%. They were equal to $p_y = 0.28 \pm 0.01$ (giving a polarization efficiency of 83%) and $p_{yy} = 0.94 \pm 0.01$ (94% efficiency), the errors being only statistical. In the second mode (the ''two-state'' mode), the beam is purely vector polarized and alternates between ''up'' and ''down'' polarization states. The value of p_y was regularly measured and found equal to 0.63 ± 0.01 giving a polarization efficiency of 95%. The ''four-state'' beam was used in order to measure the tensor analyzing power A_{yy} which appears in S_d^y. Determination of analyzing powers does not require measuring the polarization of the scattered particles, so data were taken rapidly in this phase. When enough data were acquired to determine A_{yy} for each angle and range of excitation energy to be studied, the ''four-state'' beam was discontinued. The remainder of the experiment was run using the ''two-state'' mode, which doubled the vector polarization of the incident beam. The intensity of the beam was on the order of 10^{11} deuterons per second.

Absolute cross sections were measured using two independent monitors. The ratio of the counting rates of the monitors remained constant to $\pm 6\%$ during the whole experiment. The absolute calibration of the monitors was performed with the Carbon activation method [32]. The uncertainty on the absolute cross sections is estimated at $\pm 15\%$. The uncertainty on S_d^y comes essentially from statistical errors on $K_y^{y'}$.

Good background rejection was obtained by setting horizontal and vertical windows on target and focal-plane variables of the scattered deuterons. It was shown that, for a deuteron energy of 400 MeV, POMME can cover an excitation energy range of 21 MeV.

V. EXPERIMENTAL RESULTS AND COMPARISON WITH RPA PREDICTIONS

A. Elastic $(\vec{d},\vec{d})$ scattering at 400 MeV

The cross section, vector, and tensor analyzing powers were measured with the four state polarized beam from 3 to 24° in ^{90}Zr and from 3 to 22° in ^{208}Pb. The results for ^{90}Zr and ^{208}Pb are given in Fig. 1 and Fig. 2, respectively, and are compared to the best fit optical potential calculations.

The optical potential parameters were obtained by fitting the data assuming the following shape for the potential:

$$V(r) = V_{\rm Coul} + U_R F_R(r) + iW_i F_i(r) + [V_{\rm so} G_{\rm so}(r) + iW_{\rm so} G_{\rm iso}(r)] \vec{L}\vec{S},$$

where

$$F_k(r) = \left[1 + \exp\left[\frac{r - R_k A^{1/3}}{a_k}\right]\right]^{-1},$$

with $k = R$ or i,

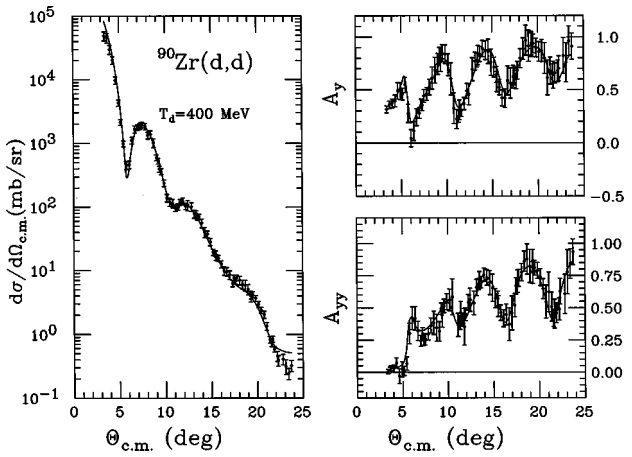

FIG. 1. The measured elastic cross sections and analyzing powers A_y and A_{yy} for ^{90}Zr compared to the *best fit* calculations obtained with the optical parameters given in Table I.

$$G_k(r)=\frac{1}{r}\frac{d}{dr}F_k(r),$$

with $k=$ so or iso.

The elastic scattering data have been analyzed with the code SEARCH [33] which can add to the $\vec{L}\vec{S}$ potential a tensor potential $(\vec{L}\vec{S})^2+\frac{1}{2}\vec{L}\vec{S}-\frac{2}{3}\vec{L}^2$ that is supposed to play a non-negligible role at intermediate energies [34]. However we found that the additional tensor term had no effect at all on the fit and therefore was ignored.

The fits of the vector asymmetry A_y and the tensor asymmetry A_{yy} are very good in both nuclei. The fit to the cross section slightly misses the oscillations at larger angles. If one forces a better fit to the cross section, it substantially degrades the fit to the asymmetries and gives unreasonably large values for the depth of the real and imaginary parts of the potential. The best fit by far is the one shown in the figures and the parameters of the optical potential for ^{90}Zr and ^{208}Pb are given respectively in Table I and Table II.

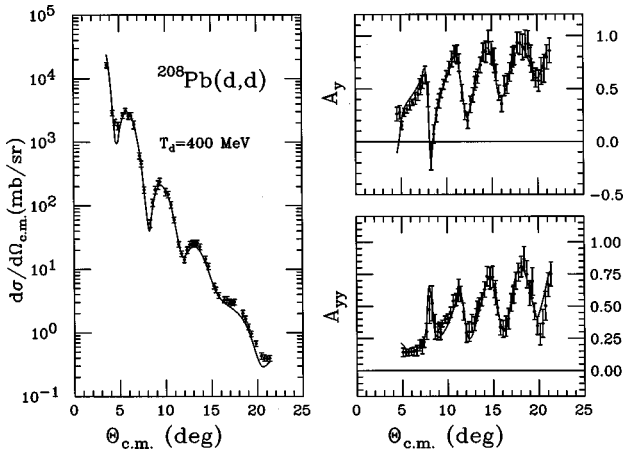

FIG. 2. The measured elastic cross sections and analyzing powers A_y and A_{yy} for ^{208}Pb compared to the *best fit* calculations obtained with the optical parameters given in Table II.

TABLE I. Optical potential parameters for 400 MeV deuteron elastic scattering on ^{90}Zr.

R_c fm	U_R MeV	R_R fm	a_R fm	W_i MeV	R_i fm	a_i fm
1.25	−21.33	1.341	0.789	−21.59	1.171	0.817
	V_{so} MeV	R_{so} fm	a_{so} fm	W_{so} MeV	R_{iso} fm	a_{iso} fm
	−4.62	1.151	0.722	2.767	1.039	0.604

B. Inelastic $(\vec{d},\vec{d}')$ scattering at 400 MeV

The measured and derived quantities are compared to DWIA/RPA predictions. The calculations have been done from 5 to 50 MeV in steps of 1 MeV of excitation energy. All multipolarities up to $J^\pi=3^+$ $(0^-,0^+,1^-,1^+,2^-,2^+,3^-,3^+)$ have been included. Higher multipolarities are not included for two reasons. First, their contributions at small momentum transfer are negligible, and, secondly the computing time becomes prohibitive with the current DWIA code. For both ^{90}Zr and ^{208}Pb, the predicted $S=0$ cross section is by far dominated by the 2^+ strength followed by the 3^- strength. The $S=1$ cross section is almost two orders of magnitude smaller and is dominated by the 2^- strength followed by the 1^+ strength. The predictions are compared to the data without any normalization factor.

1. ^{90}Zr

The analog of a spin 1^+ excitation in ^{90}Zr has been first reported in a (p,n) charge-exchange reaction at 45 MeV [35] and has been confirmed by $(^3\mathrm{He},t)$ at 80 MeV and 120 MeV [36,37]. The existence of a large 1^+ spin resonance was first observed in ^{90}Zr by 200 MeV (p,p') inelastic scattering; it is centered at 8.9 MeV with a FWHM of 1.7 MeV [38,39]. Experiments performed at 319 MeV with a polarized proton beam [40] where the analyzing power A_y and the spin-flip probability S_{nn} were also measured showed that spin excitations are present up to at least 25 MeV. This (p,p') experiment does not separate isoscalar and isovector spin-flip transitions. However, due to the relative strengths of the isovector and the isoscalar spin interactions, the observed spin strength is expected to be mainly isovector. Our motivation in studying ^{90}Zr by 400 MeV $(\vec{d},\vec{d}')$ inelastic scattering has been to search for possible $S=1$, $T=0$ strength at low excitation energy and in the continuum.

Measurements were performed at spectrometer angles of 4 and 6 °, covering the total angular range from 3 to 7 ° and

TABLE II. Optical potential parameters for 400 MeV deuteron elastic scattering on ^{208}Pb.

R_c fm	U_R MeV	R_R fm	a_R fm	W_i MeV	R_i fm	a_i fm
1.20	−12.25	1.366	0.803	−19.59	1.196	0.841
	V_{so} MeV	R_{so} fm	a_{so} fm	W_{so} MeV	R_{iso} fm	a_{iso} fm
	−2.856	1.164	0.788	0.404	1.268	0.802

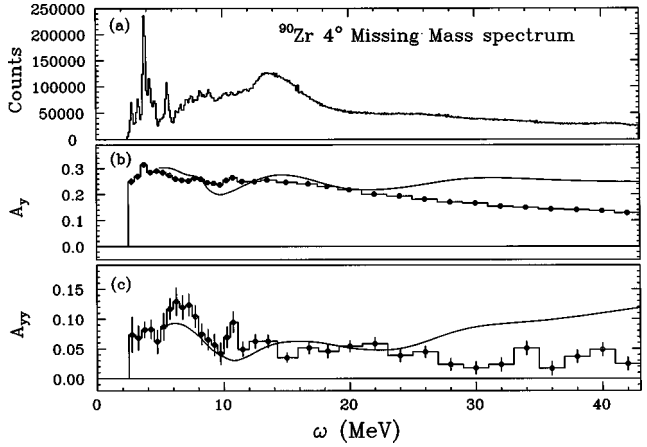

FIG. 3. Results for ^{90}Zr at 4° (lab) as a function of the excitation energy. (a) The missing mass spectrum; (b) the A_y spectrum binned in energy and compared to DWIA/RPA predictions; (c) the A_{yy} spectrum binned in energy and compared to DWIA/RPA predictions.

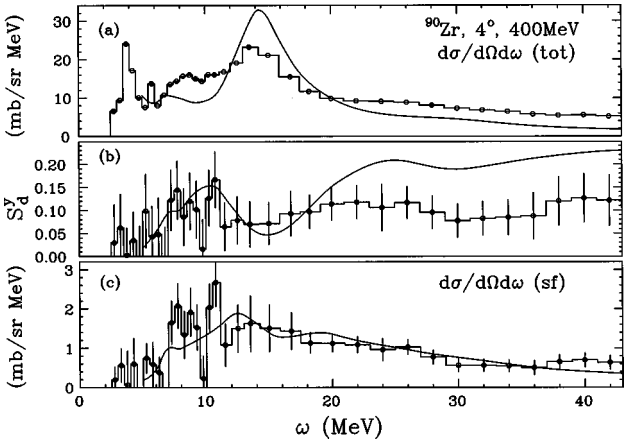

FIG. 4. Results for ^{90}Zr at 4° (lab) as a function of the excitation energy. (a) The missing mass spectrum binned in energy and normalized to give mb/sr MeV; (b) the signature S_d^y; (c) the spin-flip cross section spectrum. All spectra are compared to DWIA/RPA predictions.

the momentum transfer range from 0.28 to 0.8 fm^{-1}. The excitation range covered was from 2.5 to 43 MeV, using three different magnetic fields for the spectrometer.

a. *Directly measured quantities*. In Fig. 3(a) is given the missing mass spectrum taken at 4° with an energy resolution of 200 keV. Below 6 MeV of excitation energy, we see several discrete states with the most prominent one being the well known 2^+ state at 3.84 MeV. The known states [41] at 2.75 MeV (3^-), 3.31 MeV (2^+), and 5.59 MeV (2^+) are also clearly seen. A wide structure (possibly consisting of several overlapping structures) is seen between 6 and 10 MeV. The giant quadrupole resonance (GQR) is clearly excited around 14 MeV. The continuum above 20 MeV is smooth and decreases slowly with excitation energy. The A_y and A_{yy} spectra are respectively given in Figs. 3(b) and 3(c). These spectra have been binned in excitation energy in order to get reasonable statistical uncertainties on the measured asymmetries in each bin; the bin width increases with increasing excitation energy. The measured A_y spectrum is almost structureless; the values of A_y are positive and decrease smoothly with excitation energy. The DWIA/RPA calculation reproduces the magnitude of the asymmetry below 20 MeV but overestimates it by almost a factor of two at large excitation energies. The calculated A_y spectrum shows more structure than the measured one, especially a wide oscillation around the location of the GQR. The measured A_{yy} spectrum shows structure and relatively large positive values between 6 and 8 MeV and at 10.7 MeV. The DWIA/RPA calculation reproduces fairly well the data below 20 MeV but overestimates it in the continuum.

The raw missing mass spectrum was summed in larger size bins in order to get reasonable statistical uncertainties on the calculated signature S_d^y. The sizes of the bins are chosen in such a way as to have enough statistics in each bin while at the same time preserving as much as possible the shape of the structures. The binned missing mass spectrum at 4° is shown in Fig. 4(a). As a result of the binning, some structures are less visible than in the raw missing mass spectrum. The calculated spectrum reproduces the overall shape of the measured spectrum. The position of the GQR is correctly reproduced around 14 MeV, however too much strength is predicted in this region.

The spin-flip probability S_d^y spectrum is shown in Fig. 4(b). The signature is essentially compatible with zero for all the energy region below 7.5 MeV with the possible exception of the bin centered at 5.2 MeV. All the strong natural parity states at low excitation energies have signatures compatible with zero. This shows that even in a heavy nucleus such as ^{90}Zr, where distortion effects are not negligible, S_d^y remains a good signature. The barely nonzero value of the signature at 5.2 MeV could be due to a 1^+ state listed at 5.19 MeV in the Nuclear Data Tables [41].

From the nonzero values of S_d^y between 7 and 9.5 MeV and for the strong peak at 10.7 MeV one can conclude that some of the spin strength previously observed in this region is $T=0$. In the continuum a small enhancement of S_d^y appears between 19 and 29 MeV; it remains at a value of the order of 0.1 for the rest of the continuum up to 43 MeV. The calculated signature reproduces well the data up to 20 MeV and then overestimates it by almost a factor of two.

One way to look at possible spin-flip strength is to plot the spin-flip cross section which is just the product of the measured cross section and the signature. The spin-flip cross section spectrum is shown in Fig. 4(c). We can clearly see the concentration of spin flip strength between 7 and 9.5 MeV, in a narrow structure around 10.7 MeV and in the continuum. The DWIA/RPA calculations reproduce reasonably well the overall shape of the data above 10 MeV. The main concentration of spin-flip cross section is predicted around 12 to 14 MeV and is mainly due to 2^- strength.

The measured cross section, signature, and spin-flip cross section spectra obtained at 6° are shown in Fig. 5. The GQR is less excited, so the wide structure centered around 8 MeV is more visible in the missing mass spectrum. In the signature spectrum, the structures seen at 4° are strongly attenuated indicating a decrease of the spin-flip probability with increasing angle. The spin-flip cross section has also dropped and is less structured than at 4° with some strength left between 8 and 10 MeV, at 10.7 MeV and in the continuum.

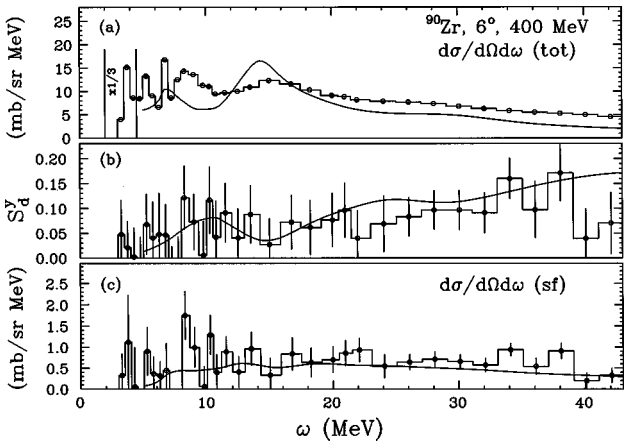

FIG. 5. Results for ^{90}Zr at 6° (lab) as a function of the excitation energy. (a) The missing mass spectrum binned in energy and normalized to give mb/sr MeV; (b) the signature S_d^y; (c) the spin-flip cross section spectrum. All spectra are compared to DWIA/RPA predictions.

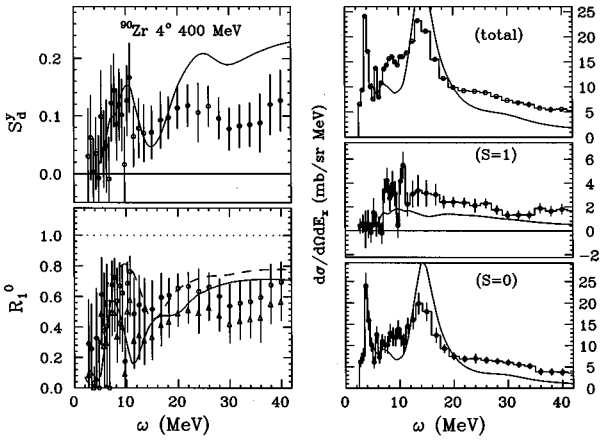

FIG. 6. Results for ^{90}Zr at 4° (lab) as a function of the excitation energy. The measured cross section is compared to the extracted $S=1$ and $S=0$ cross section on the right side of the figure. On the left side, the S_d^y spectrum is compared to the derived spin response spectrum. All spectra are compared to DWIA/RPA predictions (dashed curve corresponds to plane wave calculations).

The A_y and A_{yy} spectra are not shown here but are similar to those measured at 4°.

The calculations reproduce the overall trend of the data. The relatively fast decrease of the cross section as a function of angle for excitation energies above 10 MeV makes it difficult to measure spin observables with reasonable uncertainties. This stresses the need to make measurements at very small angles especially in heavy nuclei where distortion leads to a stronger diffractive pattern in the angular distributions.

Because of the statiscal error on S_d^y, no angular distribution could be obtained with smaller angular bins, therefore no multipolarity can be assigned to the observed excitations. However all the structures seen in the spin-flip cross section decrease with angle. The structure between 7 and 9.5 MeV is located in the same energy range as the $M1$ resonance observed in (p,p') scattering [39] and therefore this would possibly correspond to the first observation of the isoscalar component of that resonance. The 10.7 MeV spin structure has not been previously observed. The presence of higher multipolarity spin transitions cannot of course be excluded.

b. *Derived quantities*. The $S=1$ and $S=0$ cross sections have been determined from the measured quantities for deuteron scattering. As described in Sec. II, we have assumed that $\alpha^A \approx \alpha^{\text{free}}$ and used Eq. (2.5). The free value α^{free} is calculated for free *d*-nucleon scattering using the Arndt phase shifts for the nucleon-nucleon interaction [42] and a deuteron wave function which includes the *D*-state. The derived $S=1$ and $S=0$ cross-section spectra at 4° are shown in Fig. 6 together with the measured cross section for comparison. The uncertainties in the derived quantities are discussed in Ref. [15]. These uncertainties might be as large as 30% at the highest excitation energies but are small below 20 MeV.

Below 6 MeV, the $S=0$ cross section corresponds to well known natural parity states. At higher excitation energies, the spectrum is dominated by the GQR and falls off smoothly in the continuum. The DWIA/RPA calculations correctly predict the position of the GQR but give too much strength in that region and underestimate by almost a factor of two the cross section in the continuum (above 20 MeV).

The main features of the $S=1$ spectrum are essentially the same as those of the spin-flip spectrum. At low excitation energy the cross section is compatible with zero with the possible exception of the level at 5.2 MeV which as mentioned earlier could correspond to the 1^+ state at 5.19 MeV. The spectrum is dominated by two concentrations of spin strength, a 2.5 MeV wide structure centered at 8 MeV and a 1 MeV wide structure at 10.7 MeV. Additional concentration of $S=1$ strength is also observed between 12 and 18 MeV. At higher excitation energies the cross section fluctuates around an average value of 1.8 mb/sr MeV. The calculations do not reproduce the structures and underestimate the cross section at all energies. The strongest predicted 1^+ cross section (0.5 mb/sr MeV) is concentrated around 12 MeV, the predicted 2^- cross section is spread between 8 and 16 MeV with a maximum value of 1.2 mb/sr MeV.

The *experimental* values of the relative spin response $\mathcal{R}_1^0$ for ^{90}Zr are also given in Fig. 6, along with the theoretical predictions. The figure shows $\mathcal{R}_1^0$ calculated from Eq. (2.7) (open circles) using the S_d^y data (given in the figure). If we replace in Eq. (2.7) the α^{free} by the calculated DWIA/RPA α^A, we get different values of $\mathcal{R}_1^0$ also shown in the figure (triangles). The difference between these two *experimental* values of $\mathcal{R}_1^0$ are, due to the difference between α^{free} and α^A, typically 15 to 30 %. Theoretical calculations have been carried out both in plane waves (PWIA/RPA, dashed curve) and distorted waves (DWIA/RPA, solid curve).

In the low excitation energy region $\mathcal{R}_1^0$ reaches a maximum between 8 and 10 MeV indicating the dominance of isoscalar spin strength in this region. At higher energies, the relative spin response remains on the average constant around a value of the order of 0.6 for $\mathcal{R}_1^0$ calculated with α^{free}, and 0.5 for $\mathcal{R}_1^0$ calculated with α^A. Both theoretical curves nicely reproduce the shape of the *experimental* response up to about 25 MeV. Except in the region around 10 MeV, the effect of the distortion on the response is small and decreases the predicted values by $\approx$10 to 20%. The fact that

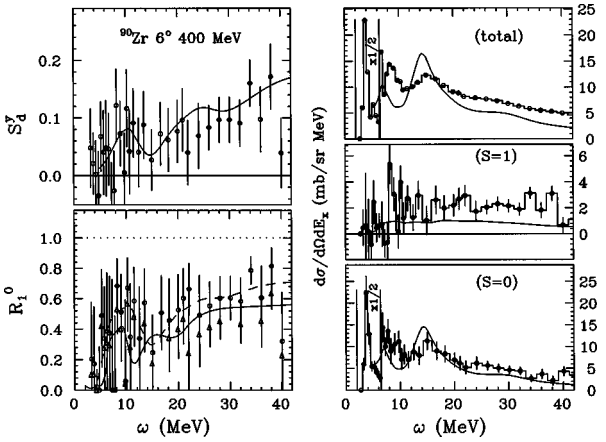

FIG. 7. Results for ^{90}Zr at 6° (lab) as a function of the excitation energy. The measured cross section is compared to the extracted $S=1$ and $S=0$ cross section on the right side of the figure. On the left side, the S_d^y spectrum is compared to the derived spin response spectrum. All spectra are compared to DWIA/RPA predictions (dashed curve corresponds to plane wave calculations).

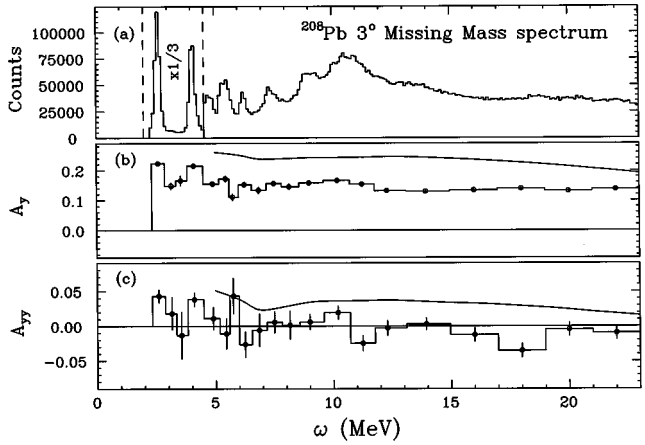

FIG. 8. Results for ^{208}Pb at 3° (lab) as a function of the excitation energy. (a) The missing mass spectrum binned in energy and normalized to give mb/sr MeV; (b) the A_y spectrum binned in energy and compared to DWIA/RPA predictions; (c) the A_{yy} spectrum binned in energy and compared to DWIA/RPA predictions.

both *experimental* responses in the continuum remain close to 0.5 is compatible with a Fermi gas type of response indicating weak collectivity in the isoscalar spin channel at these energies.

The $S=0$, $S=1$ cross sections and the relative spin responses derived at 6° are shown in Fig. 7 along with the theoretical predictions. The general pattern is similar to the results observed at 4°. In the $S=0$ spectrum, one notices the sharp decrease of the GQR which is reasonably well described by the calculation. The cross section in the continuum is still slighty underpredicted. The $S=1$ cross section has a maximum around 8 MeV and is fluctuating around 2 mb/sr MeV in the continuum. As at 4°, the $S=1$ cross section is underpredicted in the continuum. The relative spin response $\mathcal{R}_1^0$ has the same shape as at 4° and leads to the same conclusions.

2. ^{208}Pb

The concentration of 1^+ strength in ^{208}Pb was first predicted by Vergados [43] with two low energy states at 5.45 and 7.52 MeV. The low energy component is dominated by its isoscalar component and is labelled the 1^+, $T=0$ state; the high energy component is expected to be highly fragmented.

The existence of the isoscalar component was first established at 5.846 MeV by a resonance fluorescence measurement with polarized photons [44] and confirmed by different (e,e'), (p,p'), and (d,d') experiments. Due to the presence of many other states in the 7 to 10 MeV region, it has been much more difficult to localize the high energy component of the 1^+ spin excitation [45]. Spin-flip probabilities have been measured with 200 MeV proton inelastic scattering between 2 and 22 MeV showing a wide structure around 7 MeV in the signature spectrum corresponding to different multipolarities [46]. Until the present work nothing was known about isoscalar spin-flip transitions beyond the 1^+ state.

Preliminary calculations indicated that the signature will decrease rapidly with scattering angle in a heavy nucleus like ^{208}Pb. In order to be able to measure spin observables with meaningful statistical uncertaintities, special efforts were made to go to the smallest possible angle with the spectrometer while at the same time keeping the instrumental background as low as possible. Measurements were performed at spectrometer angles of 3 and 4 ° covering an angular range from 2 to 5 °. Fortunately the present experiment could be performed at such small angles with no significant experimental background. The excitation energy range covered was from 2 to 23 MeV.

a. *Directly measured quantities*. In Fig. 8(a) is given the raw missing mass spectrum at 3° which is dominated at low excitation energy by the 3^- state at 2.61 MeV and the 2^+ state at 4.09 MeV. Some smaller and wider structures are present between 5 and 9 MeV. The GQR is clearly seen centered at 10.5 MeV. Around 14 MeV, we barely see a structure in the spectrum which could correspond to the GMR. At higher excitation energies, the cross section decreases smoothly. The A_y and A_{yy} spectra are shown in Figs. 8(b) and 8(c), respectively. The A_y values are positive and almost constant accross the spectrum, with the exception of the low lying states. The DWIA/RPA calculation substantially overpredicts A_y at all energies. The values of A_{yy} fluctuate around zero with a relatively large positive values at 2.6, 4.1, and 5.8 MeV. The two first energies are those of the 3^- and 2^+ states. The 5.8 MeV bin has the largest A_{yy} value, does not correlate to any large structure in the missing mass spectrum, and could correspond to the isoscalar 1^+ state. The calculation overpredicts the asymmetry at almost all energies.

The binned missing mass, signature, and spin-flip spectra are given in Fig. 9 for 3° and in Fig. 10 for 4°. At both angles, the missing mass spectrum at large excitation energies is dominated by the GQR. The calculations predict the GQR 1 MeV lower than its actual position and, as for ^{90}Zr, overpredict its strength. At 3°, the cross section in the continuum is underpredicted. The sharp increase of the calculated cross section at low excitation energies corresponds to

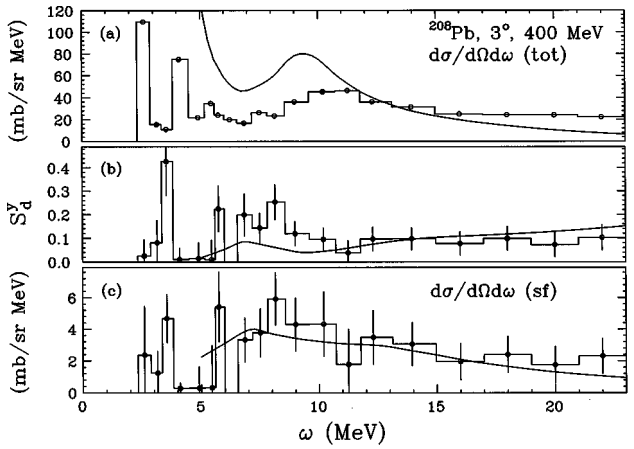

FIG. 9. Results for ^{208}Pb at 3° (lab) as a function of the excitation energy. (a) The missing mass spectrum binned in energy and normalized to give mb/sr MeV; (b) the signature S_d^y; (c) the spin-flip cross section spectrum. All spectra are compared to DWIA/RPA predictions.

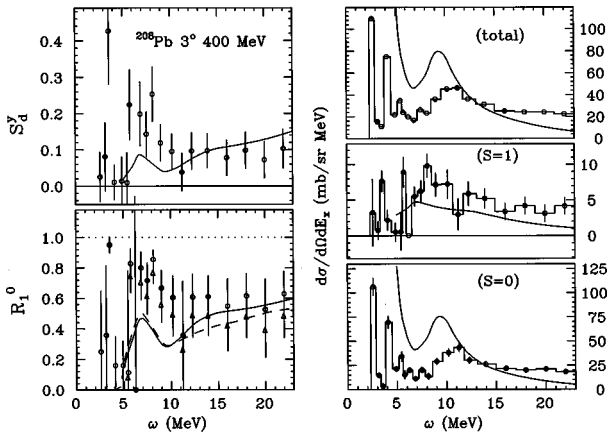

FIG. 11. Results for ^{208}Pb at 3° (lab) as a function of the excitation energy. The measured cross section is compared to the extracted $S=1$ and $S=0$ cross section on the right side of the figure. On the left side, the S_d^y spectrum is compared to the derived spin response spectrum. All spectra are compared to DWIA/RPA predictions (dashed curve corresponds to plane wave calculations).

large concentration of predicted 2^+ and 3^- strength in low lying states.

The signature spectrum at 3° is dominated by the bin at 3.5 MeV which has an average value of 0.43. This value of the signature is almost the largest possible value expected for a pure $S=1$ transition and is as large as what has been previously observed for the well known 1^+ state at 12.7 MeV in ^{12}C [15]. This impressively large value of the signature corresponds to the known 4^- spin state listed at 3.475 MeV [47]. This state is not even visible in the missing mass spectrum. This illustrates once more how powerful the S_d^y signature is in detecting spin transitions. The other relatively strong value of the signature occurs at 5.85 MeV and corresponds to the well established 1^+, $T=0$ state at 5.846 MeV. All the strong natural parity states at low excitation energy have a signature compatible with zero. Large values of S_d^y are also observed between 6.5 and 9 MeV. The signature is constant and equal to 0.1 in the continuum. The DWIA/RPA calculations reproduces well the overall shape of the spectrum. At 4°, the signatures have drastically dropped; however, the strongest values still occur at 3.5 and 5.85 MeV although with much larger error bars. The structure between 6.5 and 9 MeV is no longer visible, illustrating the importance of measurements at very small angles.

In the spin-flip cross section spectrum at 3°, the 4^- and the 1^+ states stand out very nicely; additional isoscalar strength is observed between 6 and 11 MeV. The cross section then remains constant at 2 mb/sr MeV all the way up to 23 MeV. At 4°, the spin-flip cross section has decreased; the 1^+ state is still clearly seen, but the 4^- is barely visible in the experimental tail of the large 3^- state. In the 6 to 11 MeV region, only the strength close to 10 MeV is still visible. At higher energies the cross section becomes compatible with zero. The calculations agree with the data fairly well at both angles.

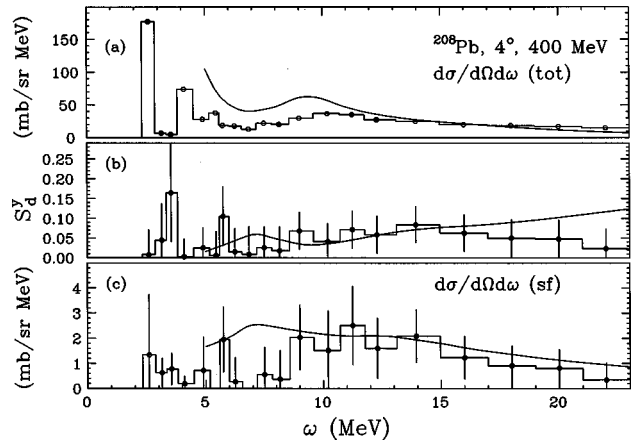

FIG. 10. Results for ^{208}Pb at 4° (lab) as a function of the excitation energy. (a) The missing mass spectrum binned in energy and normalized to give mb/sr MeV; (b) the signature S_d^y; (c) the spin-flip cross section spectrum. All spectra are compared to DWIA/RPA predictions.

b. *Derived quantities*. The derived $S=1$ and $S=0$ cross-section spectra at 3 and 4 ° are shown in Fig. 11 and Fig. 12 together with the measured cross section for comparison. As expected most of the measured cross section is $S=0$.

As in ^{90}Zr, below 6 MeV, the $S=0$ cross section corresponds to well known natural parity states. At higher excitation energies, the spectrum is dominated by the GQR and falls off smoothly in the continuum. The DWIA/RPA calculations gives the GQR 1 MeV too low and with too much strength. The strength in the continuum is again underestimated especially at 3°.

The $S=1$ spectra are essentially identical to the spin-flip spectra discussed earlier. Previously unknown isoscalar $S=1$ strength is clearly observed between 6 and 11 MeV in a region where the few spin-flip transitions observed in other reactions are essentially isovector. At 4°, the strength between 6 and 8 MeV has dropped much faster than the strength at higher energy, suggesting a low multipolarity. The calculations reproduce the overall shape of the data reasonably well. The predicted 1^+ strength around 5 to 6 MeV has a maximum value of 0.6 mb/sr MeV. The 2^- strength is predicted to be spread between 6 and 12 MeV with a maximum value of 1.7 mb/sr MeV.

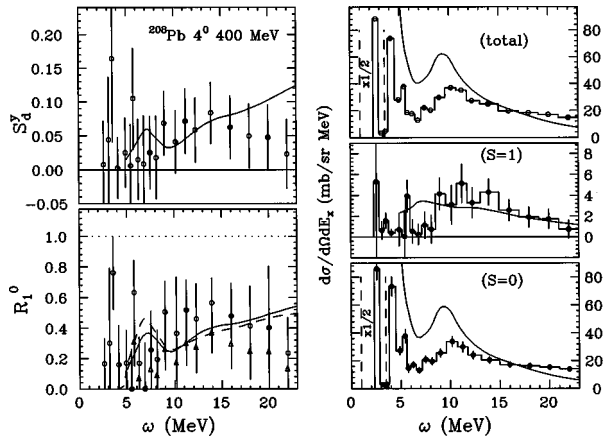

FIG. 12. Results for ^{208}Pb at 4° (lab) as a function of the excitation energy. The measured cross section is compared to the extracted $S=1$ and $S=0$ cross section on the right side of the figure. On the left side, the S_d^y spectrum is compared to the derived spin response spectrum. All spectra are compared to DWIA/RPA predictions (dashed curve corresponds to plane wave calculations).

The *experimental* values of the relative spin response $\mathcal{R}_1^0$ are also given in Fig. 11 and Fig. 12, along with the theoretical predictions. At 3°, $\mathcal{R}_1^0$ calculated with α^{free} (open circles), reaches almost 100% for the 4^- state, is of the order of 80% between 5.5 and 9 MeV and drops to 60% in the continuum. $\mathcal{R}_1^0$ calculated with α^A is only meaningful in the continuum where it fluctuates around 50%. At 3°, both theoretical curves strongly underestimate the spin response below 11 MeV but give the overall magnitude in the continuum reasonably well. The effect of the distortion on the response is small and increases the predicted values by ≈10 to 20 %. As in ^{90}Zr, the fact that both *experimental* responses in the continuum remain close to 0.5–0.6 is compatible with a Fermi gas type of response indicating a weak collectivity in the isoscalar spin channel at these energies. At 4°, except for the 4^- and 1^+ states, both experimental responses have dropped drastically, and the uncertainties are correspondingly large.

VI. SUMMARY AND CONCLUSIONS

This first attempt at mapping the isoscalar spin strength has been carried out from 2.5 to 43 MeV in ^{90}Zr and from 2 to 23 MeV in ^{208}Pb. In ^{90}Zr, we have the first evidence for localized isoscalar spin strength centered at 8 MeV (2.5 MeV wide), 10.7 MeV (1 MeV wide), and in the continuum. The 8 MeV structure seems to have a forward peaked angular distribution and quite possibly is the isoscalar component of the ''$M1$ resonance'' previously seen in (p,p') scattering. In ^{208}Pb, the already known spin states 4^- at 3.475 MeV and 1^+ state at 5.846 MeV which are barely visible in the missing mass spectrum, stand out clearly in the signature, spin-flip, and $S=1$ cross section spectra, showing once more how powerful our method is in extracting the isoscalar spin strength. A previously unknown concentration of $S=1$ strength is observed between 6 and 11 MeV with the strength between 6 and 8 MeV decreasing faster as a function of angle than the strength between 9 and 11 MeV. In both nuclei, $S=1$ strength is present uniformly in the continuum. The relative isoscalar ($T=0$) spin responses $\mathcal{R}_1^0$ have been extracted and are quite different from the relative responses determined in proton data on lighter nuclei [15] (which contain both isoscalar and isovector responses). In particular $\mathcal{R}_1^0$ values show no tendency to rise with increasing excitation energy. The fact that $\mathcal{R}_1^0$ values are of the order of 50% in the continuum confirms our previous conclusion, obtained in ^{40}Ca and ^{12}C, that the $S=1$, $T=0$ response is compatible with that of a free Fermi gas, indicating weak collectivity in the isoscalar spin channel.

Extensive microscopic DWIA/RPA calculations have been carried out for both nuclei. The RPA strength in the $S=0$, $T=0$ channel was scaled down in ^{90}Zr to preserve the sum rule in that channel. The calculations are compared to the data without any normalization. This was not the case in lighter nuclei, where for comparison with the data, the DWIA/RPA predictions had to be normalized respectively by 1/3 and 1/2 in ^{12}C and ^{40}Ca. This is puzzling because it appeared that uncertainties related to the double-folding model for deuteron-nucleus interaction, discussed in Ref. [15], were responsible for the need to renormalize the calculations. The theory systematically overpredicts the GQR strength; this has also been observed in ^{40}Ca and ^{12}C and has been discussed in Ref. [15]. The $S=0$ strength in the continuum is underpredicted (in some cases by a factor of two) and the signature is overpredicted at high excitation energies. However the spin-flip cross section (which is the product of the measured cross section and the signature) is well reproduced. One possible explanation for these observations, suggested previously for the lighter nuclei [15], is the following.

The DWIA is done assuming one step reaction inelastic scattering; however, in addition to inelastic scattering, contributions from multistep reactions are possible. We can have some two step reaction mechanism such as breakup followed by pickup but this contribution should in part be taken into account in the optical potential. Other contributions coming from $(d,d'X)$ reactions leading to multiparticle final states, are probably on the average $S=0$ and therefore explain the observed excess of $S=0$ cross section. Furthermore, this excess of non-spin-flip cross section ''dilutes the signature'' and the analyzing powers, leading to lower values of the measured S_d^y, A_y, and A_{yy} as observed.

Taking these remarks into account, the overall agreement between the theory and the data is reasonable and much better than in lighter nuclei [15].

ACKNOWLEDGMENTS

We are grateful to the technical staff of the Laboratoire National Saturne for its efficient assistance during the experiment. We would like to thank Y. Bisson, G. Chesneau, and R. Margaria for their help during the setup of the experiment. Some of the authors (C.D., F.T.B., and C.G.) were supported by grants from the National Science Foundation and the U.S. Department of Energy.

[1] J. Rapaport, T. Taddeucci, T. P. Welch, C. Gaarde, J. Larsen, D. J. Horen, E. Sugarbaker, P. Koncz, C. C. Foster, C. D. Goodman, C. A. Goulding, and T. Masterson, Nucl. Phys. **A410**, 371 (1983).

[2] J. Rapaport, R. Alarcon, B. A. Brown, C. Gaarde, J. Larsen, C. D. Goodman, C. C. Foster, D. Horen, T. Masterson, E. Sugarbaker, and T. N. Taddeucci, Nucl. Phys. **A427**, 332 (1984).

[3] J. Watson, B. D. Anderson, and R. Madey, Can. J. Phys. **65**, 566 (1987).

[4] A. Brockstedt, L. Bergvist, L. Carlen, P. Ekström, B. Jakobsson, C. Ellegaard, C. Gaarde, J. S. Larsen, C. D. Goodman, M. Bedjidian, D. Contardo, J. Y. Grossiord, A. Guichard, J. R. Pizzi, D. Bachelier, J. L. Boyard, T. Hennino, J. C. Jourdain, M. Roy-Stéphan, M. Boivin, T. Hasegawa, and P. Radvanyi, Nucl. Phys. **A530**, 571 (1991).

[5] A. Richter, in *Proceedings of the International Conference on Nuclear Physics*, Florence, Italy, 1983, edited by P. Blasi and R. A. Ricci (Tipografia Compositori, Bologna, 1983), p. 189.

[6] C. Djalali, N. Marty, M. Morlet, A. Willis, J. C. Jourdain, A. Anantaraman, G. M. Crawley, and A. Galonsky, Nucl. Phys. **A388**, 1 (1982).

[7] C. Djalali, These de doctorat d'état, Université Paris XI, Orsay, 1984.

[8] F. T. Baker, L. Bimbot, R. W. Fergerson, C. Glashausser, K. W. Jones, A. Green, K. Nakayama, and S. Nanda, Phys. Rev. C **37**, 1350 (1988).

[9] F. T. Baker, L. Bimbot, R. W. Fergerson, C. Glashausser, A. Green, K. Jones, W. G. Love, and S. Nanda, Phys. Rev. C **40**, 1877 (1989).

[10] O. Häusser, M. C. Vetterli, R. W. Fergerson, C. Glashausser, R. G. Jeppesen, R. D. Smith, R. Abegg, F. T. Baker, A. Celler, R. L. Helmer, R. Henderson, K. Hicks, M. J. Iqbal, K. P. Jackson, K. W. Jones, J. Lisantti, J. Mildenberger, C. A. Miller, R. S. Sawafta, and S. Yen, Phys. Rev. C **43**, 230 (1991).

[11] F. T. Baker, L. Bimbot, R. W. Fergerson, C. Glashausser, A. Green, O. Häusser, K. Hicks, K. W. Jones, C. A. Miller, M. C. Vetterli, R. Abegg, D. Beatty, B. Bonin, B. Castel, X. Y. Chen, V. Cupps, C. Djalali, R. Henderson, K. P. Jackson, R. G. Jeppesen, K. Nakayama, S. K. Nanda, R. S. Sawafta, and S. Yen, Phys. Rev. C **44**, 93 (1991).

[12] M. Morlet, A. Willis, J. Van de Wiele, N. Marty, J. Guillot, H. Langevin-Joliot, L. Bimbot, L. Rosier, E. Tomasi-Gustafsson, G. W. R. Edwards, R. W. Fergerson, C. Glashausser, D. Beatty, A. Green, C. Djalali, F. T. Baker, and J. C. Duchazeaubeneix, Phys. Lett. B **247**, 228 (1990).

[13] B. N. Johnson, M. Morlet, C. Djalali, F. T. Baker, L. Bimbot, C. Glashausser, J. Guillot, H. Langevin-Joliot, N. Marty, L. Rosier, E. Tomassi-Gustafsson, J. van de Wiele, and A. Willis, Phys. Rev. C **51**, 1726 (1995).

[14] M. Morlet, E. Tomasi-Gustafsson, A. Willis, J. Van de Wiele, N. Marty, C. Glashausser, B. N. Johnson, F. T. Baker, D. Beatty, L. Bimbot, C. Djalali, G. W. R. Edwards, A. Green, J. Guillot, F. Jourdan, H. Langevin-Joliot, L. Rosier, and M. Y. Youn, Phys. Rev. C **46**, 1008 (1993).

[15] F. T. Baker, L. Bimbot, C. Djalali, C. Glashausser, H. Lenske, W. G. Love, M. Morlet, E. Tomasi-Gustafsson, J. Van de Wiele, J. Wambach, and A. Willis, Phys. Rep. **289**, 235 (1997).

[16] J. van de Wiele, A. Willis, and M. Morlet, Nucl. Phys. **A588**, 829 (1995).

[17] J. Sawicki, Phys. Rev. **126**, 2231 (1962).

[18] C. Yannouleas, M. Dworzecka, and J. J. Griffin, Nucl. Phys. **A397**, 239 (1993).

[19] G. F. Bertsch, P. F. Bortignon, and R. A. Broglia, Rev. Mod. Phys. **55**, 287 (1983).

[20] J. Wambach, Rep. Prog. Phys. **51**, 989 (1988).

[21] R. D. Smith and J. Wambach, Phys. Rev. C **36**, 2704 (1987).

[22] A. B. Migdal, *Theory of Finite Fermi Systems* (Wiley, New York, 1967).

[23] C. W. DeJager, H. DeVries, and C. DeVries, At. Data Nucl. Data Tables **14**, 479 (1974).

[24] S. O. Backmann, G. E. Brown, and J. A. Niskanen, Phys. Rep. **124**, 1 (1985).

[25] R. M. Laszewski and J. Wambach, Comments Nucl. Part. Phys. **14**, 321 (1985).

[26] J. W. Negele and D. Vautherin, Phys. Rev. C **5**, 1472 (1972).

[27] R. Beurtey, *Summer School, Nuclear and Particle Physics at Intermediate Energies* (Brentwood College School, B.C. Canada, 1975); J. Saudinos, J. C. Duchazeaubeneix, C. Laspalles, and R. Chaminade, Nucl. Instrum. Methods **11**, 77 (1973).

[28] B. Bonin and J. C. Duchazeaubeneix, Commisariat à l'Energie Atomique Internal Report DPhN/Saclay No. 2526 (1989); Laboratoire National Saturne Internal Report LNS/Ph/91-32 (1991).

[29] B. Bonin, A. Boudard, H. Fanet, R. W. Fergerson, M. Garçon, C. Giorgetti, J. Habault, J. Le Meur, R. M. Lombard, J. C. Lugol, B. Mayer, J. P. Mouly, E. Tomasi-Gustafsson, J. C. Duchazeaubeneix, J. Yonnet, M. Morlet, J. Van de Wiele, A. Willis, G. Greeniaus, G. Gaillard, P. Markowitz, C. F. Perdrisat, R. Abegg, and D. A. Hutcheon, Nucl. Instrum. Methods Phys. Res. A **288**, 379 (1990).

[30] B. Bonin, A. Boudard, H. Fanet, R. W. Fergerson, M. Garçon, C. Giorgetti, J. Habault, J. Le Meur, R. M. Lombard, J. C. Lugol, B. Mayer, J. P. Mouly, E. Tomasi-Gustafsson, J. C. Duchazeaubeneix, J. Yonnet, M. Morlet, J. Van de Wiele, A. Willis, G. Greeniaus, G. Gaillard, P. Markowitz, C. F. Perdrisat, R. Abegg, and D. A. Hutcheon, Nucl. Instrum. Methods Phys. Res. A **288**, 389 (1990).

[31] J. Arvieux, S. D. Baker, A. Boudard, J. Cameron, T. Hasegawa, D. A. Hutcheon, C. Kerboul, G. Gaillard, and Nguyen Van Sen, Nucl. Instrum. Methods Phys. Res. A **273**, 48 (1988).

[32] H. Quechon, Ph.D. thesis, Université Paris XI, Orsay, 1980.

[33] J. Van de Wiele and A. Willis, Code SEARCH (1992) (unpublished).

[34] J. S. Al-Khalili, J. A. Tostevin, and R. C. Johnson, Nucl. Phys. **A514**, 649 (1990); J. S. Al-Khalili and R. C. Johnson, *ibid.* **A546**, 622 (1992); Y. Iseri, M. Tanifuji, Y. Aoki, and M. Kawai, Phys. Lett. B **265**, 207 (1991).

[35] R. R. Doering, A. Galonsky, P. M. Patterson, and G. F. Bertsh, Phys. Rev. Lett. **35**, 1691 (1975).

[36] D. Ovazza, A. Willis, M. Morlet, N. Marty, P. Martin, P. de Saintignon, and M. Buenerd, Phys. Rev. C **18**, 2438 (1978).

[37] A. Galonsky, J. P. Didelez, A. Djaleis, and W. Oebert, Phys. Lett. **74B**, 176 (1978).

[38] N. Anantaraman and G. M. Crawley, Phys. Rev. Lett. **46**, 1318 (1981).

[39] G. M. Crawley, N. Anantaraman, A. Galonsky, C. Djalali, N. Marty, M. Morlet, A. Willis, J. C. Jourdain, and P. Kitching, Phys. Rev. C **26**, 87 (1982).

[40] C. Glashausser, K. W. Jones, F. T. Baker, L. Bimbot, H. Es-

bensen, R. W. Fergerson, A. Green, S. Nanda, and R. D. Smith, Phys. Rev. Lett. **58**, 2404 (1987).
[41] L. P. Ekström and J. Lyttkens-Linden, Nucl. Data Sheets **67**, 579 (1992).
[42] R. A. Arndt *et al.*, Phys. Rev. D **28**, 97 (1983).
[43] D. Vergados, Phys. Lett. **36B**, 12 (1971).
[44] K. Wienhard, W. Naatz, A. Ruckelshausen, D. Ruck, R. K. Schneider, and R. Stock, Phys. Rev. Lett. **49**, 18 (1982).
[45] C. Djalali, N. Marty, M. Morlet, A. Willis, J. C. Jourdain, N. Anantaraman, G. M. Crawley, and A. Galonsky, Phys. Rev. C **31**, 758 (1985).
[46] J. Lisantti, E. J. Stephenson, A. D. Bacher, P. Li, R. Sawafta, P. Schawndt, S. P. Wells, S. W. Wissink, W. Unkelbach, and J. Wambach, Phys. Rev. C **44**, R1233 (1991).
[47] M. J. Martin, Nucl. Data Sheets **47**, 797 (1986).